Paraxial expansion of the wave kinetic equation for electron cyclotron beams in turbulent plasmas

Hannes Weber, Omar Maj, Emanuele Poli

Max-Planck-Institut für Plasmaphysik, Boltzmannstraße 2, 85748 Garching, Germany

E-mail: hannes.weber@ipp.mpg.de

Abstract. The paraxial WKB (beam tracing) method has proven to be very powerful for the computation of electron cyclotron (EC) beams for heating, current-drive and diagnostics applications in smooth plasma equilibria. However, fluctuation-induced beam broadening with possible concerns for ITER application has raised interest on the effect of edge density fluctuations. This issue was recently tackled through a new approach based on the wave kinetic equation (WKE) and a representation of the beam in phase-space. This method has been implemented in the WKBeam code and employed to assess the impact of fluctuations under ITER conditions.

In this work we propose to apply the paraxial technique to the wave kinetic equation. On the one hand this allows a comparison to the pWKB approach on the level of equations, clarifying the physical meaning of the WKE in phase-space and the limitations of a standard Gaussian beam in physical pace. On the other hand, we achieve a remarkable speed-up compared to WKBeam: Evolution of the beam is a direct result of a system of 11 ordinary differential equations whereas in WKBeam typically 10^5 rays are traced (Monte-Carlo approach).

In its present formulation the paraxial method applies to situations in which turbulence conserves the Gaussian beam shape, which is the case in the diffusive scattering regime. For beam and turbulence parameters chosen in accordance with this requirement we achieve good agreement with the well-benchmarked WKBeam code.

1. Introduction

The WKB ansatz and generalizations thereof are commonly used for beam tracing simulations based on the assumption that the scale length of the propagating medium is much larger than the beam wave length, as is typically the case for electron cyclotron (EC) waves in plasmas used in nuclear fusion devices. However this assumption is broken if short scale density fluctuations are accounted for, calling for a different approach. The fact that tokamaks are typically 100-1000 times larger than the wave length of EC waves would require a huge amount of points in a full-wave simulation, which is numerically extremely expensive. Moreover the difficulty that hot-plasma effects lead to integro-differential equations [1] makes such approach even more challenging. However, in the last years it has been discovered that in the next-generation tokamaks edge fluctuations could have a crucial influence on the evolution of the beam width [2], [3] with possible impact for ITER. In this work we describe the total electron density n_e with a large-scale stationary background electron density n_{e0} and describe turbulence by a stationary short-scale random fluctuation field δn_e, i.e.

$$n_e = n_{e0} + \delta n_e. \tag{1}$$

This is justified by the fact that the typical frequencies of edge turbulence are much smaller than both the wave frequency and the inverse transit time of the beam in the plasma (frozen turbulence approximation). We assume that

$$\mathbb{E}\left(\delta n_e\right) = 0 \tag{2}$$

where $\mathbb{E}\left(\cdot\right)$ denotes the ensemble average for the random scalar field δn_e.

For heating and current drive applications the beam is turned on for a long time compared to the fluctuation correlation time. Hence we are interested in the ensemble average $\mathbb{E}\left(A\right)$ of a relevant physical observable A [4] rather than in its instantaneous value.

As reviewed in section 3 a simple description of the wave field is not appropriate for such problem. A description in phase-space $z = (x, N)$ in terms of the Wigner function W may be employed. Here we make use of the dimensionless space coordinate $x = r/L$ (with L the typical variational scale length of the background medium) and the refractive index N. The function W is obtained by the Wigner transformation

$$W(x,N) = \int e^{-i\kappa N\cdot s} E\left(x+\frac{s}{2}\right) E^{\dagger}\left(x-\frac{s}{2}\right) \mathrm{d}s \tag{3}$$

with the dimensionless parameter $\kappa = \frac{\omega L}{c}$, ω the angular beam frequency and c the speed of light. For the examined situation we have $\kappa \gg 1$, referred to as semiclassical limit. The function $E(x)$ is the wave electric field.

The ensemble averaged expectation value $\mathbb{E}\left(A\right)$ is deduced from the Wigner function via

$$\mathbb{E}\left(A\right) = \left(\frac{\kappa}{2\pi}\right)^2 \int A(z) W(z) \mathrm{d}z, \tag{4}$$

where $A(z)$ is the Weyl symbol corresponding to operator A.

In the WKBeam code [5] the evolution of the Wigner function is described by the wave kinetic equation (WKE) and solved numerically using a Monte-Carlo technique: Rays are randomly initialized following as probability distribution the Wigner function on the antenna plane and traced. Each ray carries a contribution to the Wigner function such that the whole beam is covered by rays. This technique is a sort of brute force approach as it requires tracing a large number of rays in order to recover the diffracting pattern of the beam. This work is a first attempt to overcome this limitation by means of a paraxial expansion of the Wigner function [6] such that the beam is traced as a whole. Fluctuations are treated in the diffusive limit. We first present the theory followed by two simple test cases. The results are compared to WKBeam. We consider two-dimensional space only, which is a technical simplification and may be generalized straight forwardly.

2. Description of the beam in terms of a boundary value problem

The starting point for the phase-space description of the beam is similar to WKBeam as derived in [7]. Mathematically we consider the following boundary value problem:

$$H(z)W(z) = 0, \tag{5a}$$

$$\{H(z), W(z)\} = \mathcal{S}(W)(z), \tag{5b}$$

$$W(z)|_{\mathrm{Aps}} = \text{known boundary value}, \tag{5c}$$

with $\{\cdot,\cdot\}$ the canonical Poisson brackets, H the geometrical optics Hamiltonian derived from the relevant wave equation and $\mathcal{S}$ an integral operator describing scattering by density fluctuations. The boundary value is given on a plane Aps in phase-space which extends the physical antenna/mirror system launching the beam, as shown in figure 1.

Equation (5a) accounts for the dispersion relation, singularly limiting the support of the Wigner function to the hyper-surface $H(x, N) = 0$, which is referred to as dispersion surface. Equation (5b) is the WKE and describes the evolution of the Wigner function along the beam propagation. Equation (5c) is the boundary condition, used in order to initialize the beam. The

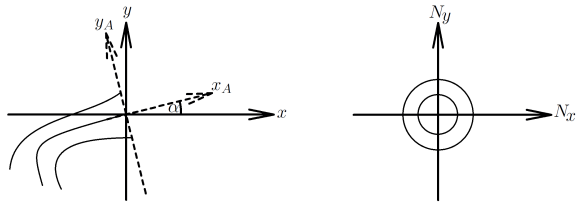

Figure 1. Phase-space (x, y, N_x, N_y) coordinate system. Left: Space coordinates (x, y) with a rotated coordinate system (x_A, y_A) aligned to the antenna plane, defined by $x_A = 0$. Right: Refractive index coordinates (N_x, N_y). An example beam launched to the lower left in physical space is shown.

boundary value is known from the electric field on the antenna plane. In the following we explore the possibility of solving equations (5) with a paraxial expansion.

2.1. Paraxial expansion of the wave kinetic equation

In the paraxial expansion it is convenient to single out the singular factor of W due to the dispersion relation (5a). We write

$$W(z) = \delta\left(H(z)\right)\tilde{W}(z), \tag{6}$$

where $\tilde{W}$ is a smooth function. In [7] we show that the WKE may be reformulated for such regularized function, with the result

$$\begin{aligned}\left\{H(z), \tilde{W}(z)\right\} =& 2\pi \int \Gamma\left(x, N, N'\right)\delta\left(H(x, N')\right) \\ &\times\left[\tilde{W}(x, N') - \tilde{W}(x, N)\right]\mathrm{d}N'.\end{aligned} \tag{7}$$

The right-hand side of equation (7) defines a scattering operator $\tilde{S}\big(\tilde{W}\big)$ in terms of the function Γ which only depends on the two-point correlation function of density fluctuations.

We search for solutions of the form

$$\tilde{W}(z) = a(\tau)e^{-\frac{\kappa}{2}G_{ij}(\tau)\eta_i\eta_j}, \tag{8}$$

where (τ, η) are phase-space coordinates aligned to the beam and defined as follows: The center of the beam (referred to as "reference ray") is found for $\eta = 0$: The corresponding Cartesian phase-space coordinates $\mathcal{Z} = (\mathcal{X}, \mathcal{Y}, \mathcal{N}_x, \mathcal{N}_y)$ are constructed upon making use of Hamilton's equations of motion

$$\frac{\mathrm{d}\mathcal{Z}_n}{\mathrm{d}\tau} = \Omega_{mn}\frac{\partial H}{\partial z_m} \quad \text{with} \quad \Omega = \begin{pmatrix} 0 & -\mathbb{1} \\ \mathbb{1} & 0 \end{pmatrix}, \tag{9}$$

with initial conditions such that $H\big(\mathcal{Z}(0)\big) = 0$. Here and throughout the paper, the sum over repeated indices is implied. The coordinates perpendicular to the propagation of the reference ray are combined in the vector η: We have $\eta = (y, N_\tau, N_y)$ with y the space coordinate perpendicular to beam propagation, N_τ the refractive index in direction of refractive index evolution, $\mathrm{d}\mathcal{N}/\mathrm{d}\tau$, and N_y the refractive index perpendicular to N_τ.

If we introduce the direction vectors e_y, e_{N_τ}, and e_{N_y} along the y-, N_τ-, and N_y-directions, respectively, we have the transformation

$$\begin{aligned}z(\tau, \eta) = \mathcal{Z}(\tau) + e_y(\tau)y + e_{N_\tau}(\tau)N_\tau \\ + e_{N_y}(\tau)N_y.\end{aligned} \tag{10}$$

It can be analytically shown that

$$\eta_1^m\eta_2^n\eta_3^k e^{-\frac{\kappa}{2}G_{ij}(\tau)\eta_i\eta_j} = \mathcal{O}\big(\kappa^{-(m+n+k)/2}\big). \tag{11}$$

For this reason high-order terms in η are suppressed when multiplied with $\tilde{W}$ involving the exponential. The idea of paraxial expansion is hence to insert ansatz (8) into the WKE and separate different orders of κ in order to derive phase-space beam tracing equations, accounting for (11).

As a starting point the WKE (7) is formulated in terms of the beam coordinates

$$\begin{aligned}\frac{\partial H(z)}{\partial z_m}(\eta)\Omega_{mn}\left[\frac{\partial(\tau,\eta)}{\partial z}(\eta)\frac{\partial\tilde{W}}{\partial(\tau,\eta)}(\eta)\right]_n \\ = \tilde{S}\big(\tilde{W}\big)(\eta).\end{aligned} \tag{12}$$

The functions $\partial H/\partial z_m$ and $\partial(\tau, \eta)/\partial z$ written in terms of (τ, η) are expanded around $\eta = 0$ up to first order and ansatz (8) is inserted so that on the left-hand side different orders in η are exposed with the result that

$$\begin{aligned}&\left[\frac{\partial H}{\partial z_m} + \frac{\partial^2 H}{\partial z_m \partial z_b}\frac{\partial z_b}{\partial \eta_k}\eta_k\right]\Omega_{mn} \\ &\left\{\left[\frac{\partial\tau}{\partial z_n} + \frac{\partial}{\partial\eta_d}\left(\frac{\partial\tau}{\partial z_n}\right)\eta_d\right]\left[\frac{\partial a/\partial\tau}{a} - \frac{\kappa}{2}\frac{\partial G_{ij}}{\partial\tau}\eta_i\eta_j\right]\right. \\ &\left.-\frac{\kappa}{2}\left[\frac{\partial\eta_a}{\partial z_n} + \frac{\partial}{\partial\eta_e}\left(\frac{\partial\eta_a}{\partial z_n}\right)\eta_e\right]\left[G_{aj}\eta_j + \eta_i G_{ia}\right]\right\}\tilde{W}(\eta) \\ &= \tilde{S}\big(\tilde{W}\big)(\eta).\end{aligned} \tag{13}$$

The functions are meant to be evaluated at $\eta = 0$ if no argument is indicated.

We observe that

$$\left.\frac{\partial H}{\partial z_m}\Omega_{mn}\frac{\partial\tau}{\partial z_n}\right|_{\eta=0} = \frac{\partial\tau}{\partial\tau} = 1,$$

and analogously,

$$\left.\frac{\partial H}{\partial z_m}\Omega_{mn}\frac{\partial\eta}{\partial z_n}\right|_{\eta=0} = \frac{\partial\eta}{\partial\tau} = 0.$$

Therefore

$$-\frac{\kappa}{2}\frac{\partial H}{\partial z_m}\Omega_{mn}\frac{\partial\eta_a}{\partial z_n}\left[G_{ai} + G_{ia}\right]\eta_i\tilde{W} = 0 \tag{14}$$

identically for any non-trivial matrix G. The leading terms are of $\mathcal{O}(1)$ and accepting a remainder of $\mathcal{O}(\kappa^{-1/2})$ yields

$$\begin{aligned}&\frac{\partial a/\partial\tau}{a} - \frac{\kappa}{2}\frac{\partial G_{ij}}{\partial\tau}\eta_i\eta_j \\ &- \frac{\kappa}{2}\frac{\mathrm{d}\mathcal{Z}_n}{\mathrm{d}\tau}\left[\frac{\partial}{\partial\eta_j}\left(\frac{\partial\eta_a}{\partial z_n}\right)G_{ai} + \frac{\partial}{\partial\eta_i}\left(\frac{\partial\eta_a}{\partial z_n}\right)G_{aj}\right] \\ &- \frac{\kappa}{2}\frac{\partial^2 H}{\partial z_m\partial z_b}\frac{\partial\eta_a}{\partial z_n}\left[\frac{\partial z_b}{\partial\eta_j}G_{ai} + \frac{\partial z_b}{\partial\eta_i}G_{aj}\right]\tilde{W}(\eta)\eta_i\eta_j \\ &+ O(\kappa^{-1/2}) = \tilde{S}\big(\tilde{W}\big)(\eta) \end{aligned} \tag{15}$$

where the symmetry of G has been accounted for.

The right-hand side still needs to be evaluated. We consider the diffusive limit in this work, described by Taylor expanding the function $\tilde{W}$ in $\tilde{S}\big(\tilde{W}\big)$ around η up to second order. Such approach allows us to compute analytically the integral in (7). The result reads

$$\begin{aligned}\tilde{S}\left(\tilde{W}\right)(\tau,\eta) = \mathcal{D}_{\alpha\beta}\Big\{ &- \frac{\kappa}{2}\left(G_{\alpha\beta} + G_{\beta\alpha}\right) \\ &+ \frac{\kappa^2}{4}\left(G_{\alpha i} + G_{i\alpha}\right)\left(G_{\beta j} + G_{j\beta}\right)\eta_i\eta_j\Big\}\tilde{W}(\eta)\end{aligned} \tag{16}$$

with the diffusion coefficient

$$\begin{aligned}\mathcal{D}_{\alpha\beta} = \pi\int &\Gamma\left(x,N,N'\right)\delta\left(H(x,N')\right) \\ &\times\left(\eta'_\alpha - \eta_\alpha\right)\left(\eta'_\beta - \eta_\beta\right)\mathrm{d}N'\end{aligned} \tag{17}$$

and α, β running on $2,3$ (refractive index components) only. Split into different power of η equation (15) reads

$$\frac{\partial a/\partial\tau}{a} = -\frac{\kappa}{2}\mathcal{D}_{\alpha\beta}\left(G_{\alpha\beta} + G_{\beta\alpha}\right), \tag{18a}$$

$$\begin{aligned}&\frac{\partial G_{ij}}{\partial\tau} + \frac{\mathrm{d}\mathcal{Z}_n}{\mathrm{d}\tau}\left[\frac{\partial}{\partial\eta_i}\left(\frac{\partial\eta_a}{\partial z_n}\right)G_{aj} + \frac{\partial}{\partial\eta_j}\left(\frac{\partial\eta_a}{\partial z_n}\right)G_{ia}\right] \\ &\quad + \frac{\partial^2 H}{\partial z_m\partial z_b}\Omega_{mn}\frac{\partial\eta_a}{\partial z_n}\left[\frac{\partial z_b}{\partial\eta_i}G_{aj} + \frac{\partial z_b}{\partial\eta_j}G_{ia}\right] \\ &\quad = -\frac{\kappa}{2}\mathcal{D}_{\alpha\beta}\left(G_{\alpha i} + G_{i\alpha}\right)\left(G_{\beta j} + G_{j\beta}\right).\end{aligned} \tag{18b}$$

The first of these equations is the amplitude transport equation describing the evolution of the amplitude function $a(\tau)$ along the beam. The second equation describes the evolution of the G-matrix and is such that the symmetry of G is conserved.

2.2. Initial condition

For a Gaussian wave electric field with curvature radius $R(0)$ and beam width $w(0)$ on the antenna plane,

$$E(x_A, y_A) \propto e^{-\frac{y_A^2}{w(0)^2} - \frac{i\kappa y_A^2}{2R(0)}}, \tag{19}$$

lifted to phase-space via (3) and compared to the Gaussian ansatz (8) we find as initial condition (i.e. for $\tau = 0$) for the G-matrix components

$$G_{11}(0) = \frac{4}{\kappa w^2} + \frac{\kappa w^2}{R^2}, \tag{20a}$$

$$G_{12}(0) = \frac{\kappa w^2}{R}\frac{\mathcal{N}_y}{\mathcal{N}}, \tag{20b}$$

$$G_{13}(0) = -\frac{\kappa w^2}{R}\frac{\mathcal{N}_x}{\mathcal{N}}, \tag{20c}$$

$$G_{22}(0) = \kappa w^2\frac{\mathcal{N}_y^2}{\mathcal{N}^2}, \tag{20d}$$

$$G_{23}(0) = -\kappa w^2\frac{\mathcal{N}_x\mathcal{N}_y}{\mathcal{N}^2}, \tag{20e}$$

$$G_{33}(0) = \kappa w^2\frac{\mathcal{N}_x^2}{\mathcal{N}^2}, \tag{20f}$$

where $\left(\mathcal{N}_x, \mathcal{N}_y\right)$ are the Cartesian components of the refractive index vector on the initial point of the reference ray and $\mathcal{N}^2 = \mathcal{N}_x^2 + \mathcal{N}_y^2$.

2.3. Computation of the wave field energy density

The electric field energy density $W_E(x)$ at the spatial position x is obtained by

$$W_E(x) = \left(\frac{\kappa}{2\pi}\right)^2\int W(x,N)dN,$$

which can be formally considered a special choice of the observable A in equation (4), cf. Ref. [7]. The Gaussian ansatz (8) allows the analytical computation of the involved integral for $\eta_2,\ \eta_3 \ll \mathcal{N}$, with the result

$$\begin{aligned}W_E(\tau, y) = &\sqrt{\frac{\pi}{2\kappa\left(G_{22}\mathcal{N}_y^2 - 2G_{23}\mathcal{N}_x\mathcal{N}_y + G_{33}\mathcal{N}_x^2\right)}} \\ &\times e^{-\frac{\kappa}{2}\left[G_{11} - \frac{\left(G_{12}\mathcal{N}_y - G_{13}\mathcal{N}_x\right)^2}{G_{22}\mathcal{N}_y^2 - 2G_{23}\mathcal{N}_x\mathcal{N}_y + G_{33}\mathcal{N}_x^2}\right]y^2}.\end{aligned} \tag{21}$$

3. Wave field versus phase-space description

The paraxial WKB ansatz [8] for the wave electric field is widely employed in the field of EC wave propagation in plasmas and we refer to the TORBEAM code [9, 10] as an example. Such description in terms of the wave field is close to Maxwell's equations and, therefore, quite natural for the problem of wave propagation. However it is not suitable for the problem of an ensemble averaged beam under the presence of fluctuations, which we describe in phase-space in this work. We explore the difference of the two descriptions in this section. To work out the essential point we analyze a simple example: We study a beam propagating in negative x-direction with $\mathcal{Y} = \mathcal{N}_y = 0$: With such choice the x-coordinate may be seen as a parameter of propagation and the beam shape is purely

described in y-direction, which allows to restrict the analysis to y-direction.

For the described case the paraxial WKB ansatz for the electric field reads

$$E(y) \propto e^{-\frac{y^2}{w^2} - i\kappa\frac{y^2}{2R}} \tag{22}$$

with w the beam width and R the curvature radius. Treating x as a parameter and lifting to phase-space in y-direction via the Wigner transformation (3) yields

$$\tilde{W}_p(y, N_y) \propto e^{-\left(\frac{2}{w^2} + \frac{\kappa^2 w^2}{8R^2}\right)y^2 - \frac{\kappa^2 w^2}{2R} y N_y - \frac{\kappa^2 w^2}{2} N_y^2}. \tag{23}$$

On the other hand the y-dependency in ansatz (8) for the case under consideration is

$$\tilde{W}(y, N_y) \propto e^{-\frac{\kappa}{2}\left[G_{11}y^2 + 2G_{13}yN_y + G_{33}N_y^2\right]}. \tag{24}$$

As will be seen in section 4.2 for propagation in x-direction $G_{ij} = 0$ for $i = 2$ or $j = 2$. Direct comparison clearly shows that in (24) we find more degrees of freedom than in (23): In the exponential the y^2-, the yN_y- and the N_y^2-terms have independent prefactors, whereas the wave field lifted to phase-space has the two parameters w and R only.

The ansatz used in this work can describe more general phase-space distributions than those obtained from a Gaussian wave beam. In practice this means that the average Wigner distribution, in general, does not correspond to the Wigner transform of any given wave field. We rather need to interpret the averaged Wigner distribution as a mathematical object which is used to deduce averaged expectation values as defined in (4) and which describes the beam "feeling" the whole ensemble of fluctuations.

Such problems are better known in the field of statistical quantum mechanics, as reviewed in [11]: The cases which may be described in terms of a wave function are called "pure states", as opposed to the more general "mixed states".

As a criterion to decide whether we are dealing with a pure or a mixed wave electric field we associate to the Wigner function $\tilde{W}(y, N_y)$ the entropy S measuring the "purity" as defined in [12]:

$$S(x) = 1 - \frac{2\pi}{\kappa} \frac{\int \tilde{W}^2(y, N_y)\mathrm{d}y\mathrm{d}N_y}{\left(\int \tilde{W}(y, N_y)\mathrm{d}y\mathrm{d}N_y\right)^2}. \tag{25}$$

For pure fields one has $S = 0$ and for mixed fields $0 < S < 1$. As an example one can insert the Wigner function $\tilde{W}_p$ (23), which gives $S = 0$ as a result, in contrast to the Wigner function $\tilde{W}$ (24), which leads to

$$S = 1 - \frac{1}{2}\sqrt{G_{11}G_{33} - G_{13}^2}. \tag{26}$$

With the initial conditions (20) one has $S = 0$ on the antenna plane. This means that, still, we start with a pure wave beam. However it may get mixed by fluctuations, as in the example in section 4.2.

4. Specific toy models

In this section as an example we study the propagation of the beam for two simple toy models. The reader should be warned that, unlike the previous part, physical units are used, e.g. lengths are measured in cm and not normalized with the scale length L.

4.1. Linear layer, no fluctuations

We study the so-called model of a linear layer, which has a linearly decreasing refractive index when moving in direction of the negative x-axis with scale length L, leading to the Hamiltonian

$$H(x, N) = N^2 - 1 + \frac{x}{L}. \tag{27}$$

We consider the unperturbed beam for the moment, i.e. $\mathcal{D}_{\alpha\beta} = 0$. We show how, starting with such Hamilton function, the beam tracing equations in phase space may be derived.

In accordance with section 2.1 we define the direction vectors

$$e_y = \begin{pmatrix} -\mathcal{N}_y/\mathcal{N} \\ \mathcal{N}_x/\mathcal{N} \\ 0 \\ 0 \end{pmatrix}, \; e_{N_\tau} = \begin{pmatrix} 0 \\ 0 \\ 1 \\ 0 \end{pmatrix}, \; e_{N_y} = \begin{pmatrix} 0 \\ 0 \\ 0 \\ 1 \end{pmatrix}, \tag{28}$$

leading to the Jacobian matrix

$$\begin{aligned} \frac{\partial(\tau, \eta)}{\partial z}(\eta) = &\begin{pmatrix} \frac{\mathcal{N}_x}{2\mathcal{N}^2} & \frac{\mathcal{N}_y}{2\mathcal{N}^2} & 0 & 0 \\ -\frac{\mathcal{N}_y}{\mathcal{N}} & \frac{\mathcal{N}_x}{\mathcal{N}} & 0 & 0 \\ \frac{\mathcal{N}_x}{2L\mathcal{N}^2} & \frac{\mathcal{N}_y}{2L\mathcal{N}^2} & 1 & 0 \\ 0 & 0 & 0 & 1 \end{pmatrix} \\ &+ \begin{pmatrix} \frac{\mathcal{N}_x\mathcal{N}_y}{4L\mathcal{N}^5} & \frac{\mathcal{N}_y^2}{4L\mathcal{N}^5} & 0 & 0 \\ 0 & 0 & 0 & 0 \\ \frac{\mathcal{N}_x\mathcal{N}_y}{4L^2\mathcal{N}^5} & \frac{\mathcal{N}_y^2}{4L^2\mathcal{N}^5} & 0 & 0 \\ 0 & 0 & 0 & 0 \end{pmatrix} y. \end{aligned} \tag{29}$$

The first expression on the right hand side contains $\frac{\partial\eta}{\partial z}$ evaluated on the center of the beam, whereas the second expression is linear in η, more specifically in the $\eta_1 = y$ component, yielding the first order $\frac{\partial}{\partial\eta_i}\left(\frac{\partial\eta}{\partial z}\right)$ correction. Explicitly evaluating equation (18b) for these expressions leads to the following

evolution equations for the G-components:

$$\frac{\partial G_{11}}{\partial \tau} = -\frac{\mathcal{N}_y}{L^2\mathcal{N}^3}G_{12}, \tag{30a}$$

$$\frac{\partial G_{12}}{\partial \tau} = -2\frac{\mathcal{N}_y}{\mathcal{N}}G_{11} + \frac{\mathcal{N}_x}{L\mathcal{N}^2}G_{12} - \frac{\mathcal{N}_y}{2L^2\mathcal{N}^3}G_{12}, \tag{30b}$$

$$\frac{\partial G_{13}}{\partial \tau} = +2\frac{\mathcal{N}_x}{\mathcal{N}}G_{11} + \frac{\mathcal{N}_y}{L\mathcal{N}^2}G_{12} - \frac{\mathcal{N}_y}{2L^2\mathcal{N}^3}G_{13}, \tag{30c}$$

$$\frac{\partial G_{22}}{\partial \tau} = -4\frac{\mathcal{N}_y}{\mathcal{N}}G_{12} + 2\frac{\mathcal{N}_x}{L\mathcal{N}^2}G_{22}, \tag{30d}$$

$$\frac{\partial G_{23}}{\partial \tau} = +2\frac{\mathcal{N}_x}{\mathcal{N}}G_{12} - 2\frac{\mathcal{N}_y}{\mathcal{N}}G_{13} + \frac{\mathcal{N}_y}{L\mathcal{N}^2}G_{22} + \frac{\mathcal{N}_x}{L\mathcal{N}^2}G_{23}, \tag{30e}$$

$$\frac{\partial G_{33}}{\partial \tau} = +4\frac{\mathcal{N}_x}{\mathcal{N}}G_{13} + 2\frac{\mathcal{N}_y}{L\mathcal{N}^2}G_{22}. \tag{30f}$$

In figure 2 the comparison of the paraxial ansatz to WKBeam is shown and both results match well. In figure 3 a beam with a slightly shorter focal radius but a larger beam width is considered and we see an inaccuracy of the paraxial solution. This inaccuracy is an open issue of our work in progress and needs to be better understood.

4.2. Free space plus fluctuations

In order to test fluctuations we choose free space and propagation in negative x-direction (i.e. $\mathcal{N}_x = -1$ and $\mathcal{N}_y = 0$). We add random density fluctuations with a Gaussian spectrum of the two-point correlation function

$$\Gamma(x, N, N') = \frac{\delta^2\kappa^3 L_F^2}{2\pi} e^{-\frac{\kappa^2 L_F^2}{2}\left(N'-N\right)^2} \tag{31}$$

where δ is a parameter indicating how strong fluctuations are, L_F is the fluctuation correlation length and $N = (N_x, N_y)$, $N' = \left(N'_x, N'_y\right)$. We suppose that $\delta^2 \propto \mathcal{O}\left(\kappa^{-1}\right)$ (i.e. weak fluctuations) such that the right hand side of equations (18b) is of order 1. With such model the diffusion coefficient integral (17) may be computed analytically, with the result that

$$\mathcal{D}_{22} = \frac{\pi^{1/2}\delta^2\mathcal{N}_y^2}{2^{3/2}L_F\mathcal{N}^3}, \quad \mathcal{D}_{33} = \frac{\pi^{1/2}\delta^2\mathcal{N}_x^2}{2^{3/2}L_F\mathcal{N}^3}. \tag{32}$$

The off-diagonal terms vanish, i.e. $\mathcal{D}_{23} = \mathcal{D}_{32} = 0$.

Taking into account the initial conditions (20) for $\mathcal{N}_y = 0$ the amplitude transport equation (18a) and the evolution equations for G (18b) amount to

$$\frac{\partial a}{\partial \tau} = -\kappa\mathcal{D}_{33}aG_{33}, \tag{33a}$$

$$\frac{\partial G_{11}}{\partial \tau} = -2\kappa\mathcal{D}_{33}\left(G_{13}\right)^2, \tag{33b}$$

$$\frac{\partial G_{13}}{\partial \tau} = +2G_{11} - 2\kappa\mathcal{D}_{33}G_{12}G_{33}, \tag{33c}$$

$$\frac{\partial G_{33}}{\partial \tau} = +4G_{13} - 2\kappa\mathcal{D}_{33}\left(G_{33}\right)^2, \tag{33d}$$

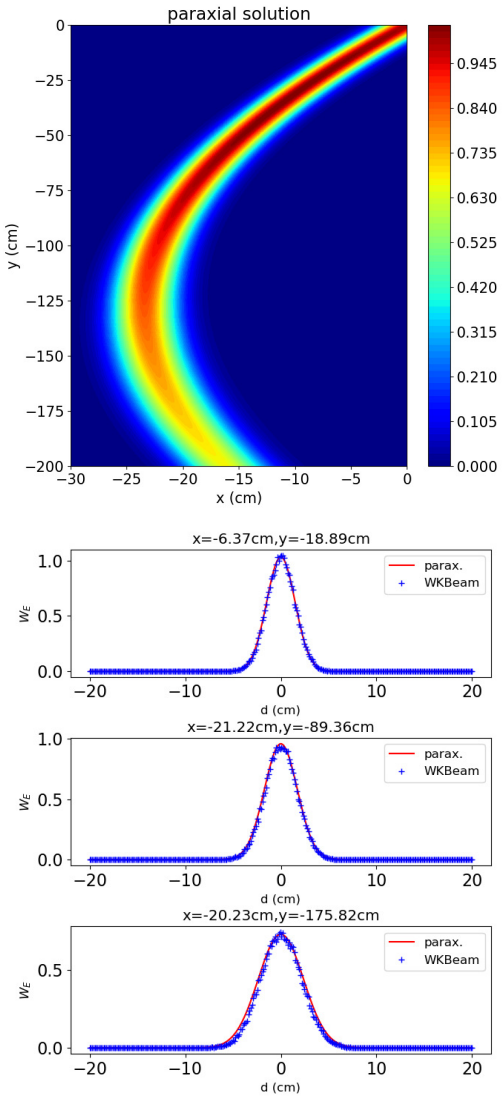

Figure 2. Initial beam width $w(0) = 3\,\mathrm{cm}$, initial beam curvature $R(0) = -1000\,\mathrm{cm}$, beam frequency $f = 140\,\mathrm{GHz}$, injection angle $\alpha = -70\,^\circ$, scale length $L = 200\,\mathrm{cm}$. Top: Energy density of the paraxial solution, below: comparison to WKBeam at selected points of the beam.

where $G_{12} = G_{22} = G_{23} = 0$, identically in τ. We run the simulation for two sets of parameters, with the results shown in figures 4 and 5. From the simulation based on the paraxial expansion of the WKE the beam width is immediately available from the G matrix whereas it is estimated via a Gauss fit from the WKBeam results. The results in figure 4 do not properly match, which is due to the fact that the choice of parameters makes the diffusive limit inappropriate [3, 7]. The results in figure 5 perfectly fit. For both it is clearly seen how entropy (26) increases when the beam propagates towards negative x-direction, starting from $S = 0$ on the antenna plane, which shows that we are

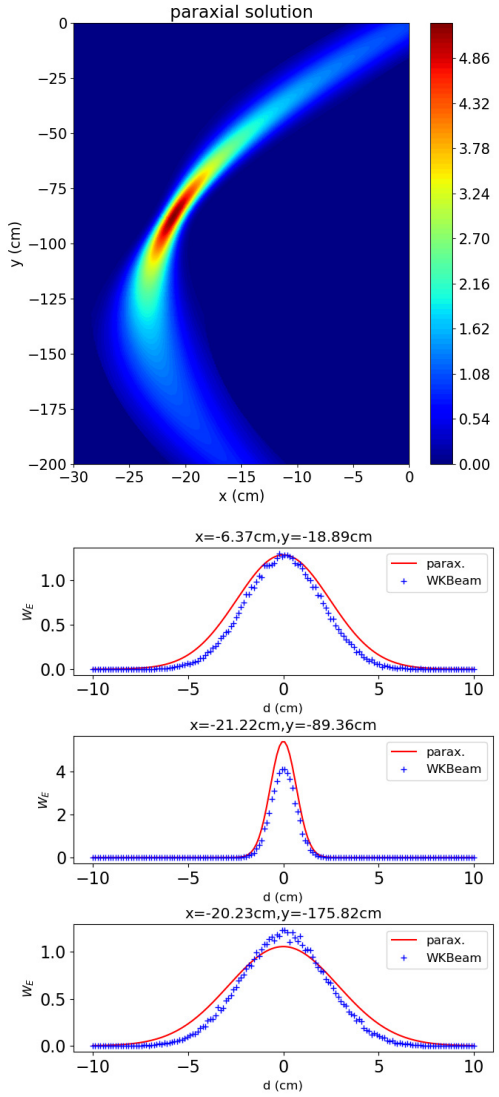

Figure 3. Initial beam width $w(0) = 5\,\mathrm{cm}$, initial beam curvature $R(0) = -100\,\mathrm{cm}$, beam frequency $f = 140\,\mathrm{GHz}$, injection angle $\alpha = -70\,^\circ$, scale length $L = 200\,\mathrm{cm}$. Top: Energy density of the paraxial solution, below: comparison to WKBeam at selected points of the beam.

dealing with mixed fields. The evolution of the entropy may be computed analytically for this simple case by inserting the evolution equations (33) in (26), with the result

$$\frac{\mathrm{d}S}{\mathrm{d}\tau} = \frac{\kappa \mathcal{D}_{33}}{2} G_{33} \sqrt{G_{11} G_{33} - G_{13}^2}. \tag{34}$$

Without fluctuations, i.e. for $\mathcal{D}_{33} = 0$, this shows that entropy does not change during beam propagation, which means that we are dealing with pure wave fields, making the wave field description appropriate.

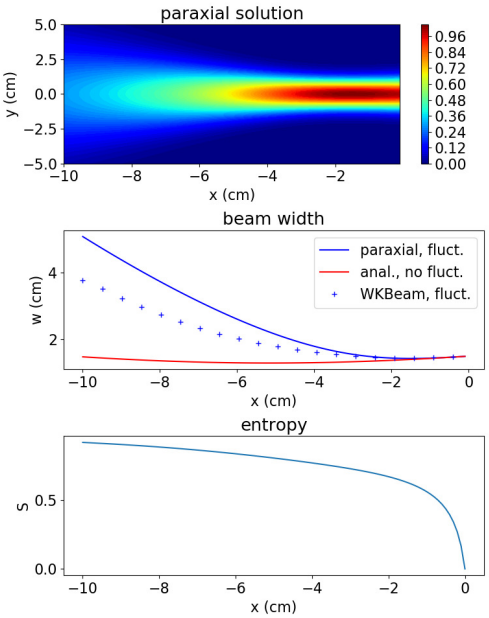

Figure 4. Initial beam width $w(0) = 1.5\,\mathrm{cm}$, initial beam curvature $R(0) = -20\,\mathrm{cm}$, beam frequency $f = 50\,\mathrm{GHz}$, fluctuation level $\delta = 0.1$, $L_F = 0.35\,\mathrm{cm}$. Top: Energy density of the paraxial solution, middle: comparison of the beam width of an analytical reference solution without fluctuation, WKBeam and the paraxial ansatz, bottom: entropy of the paraxial solution resolved in x.

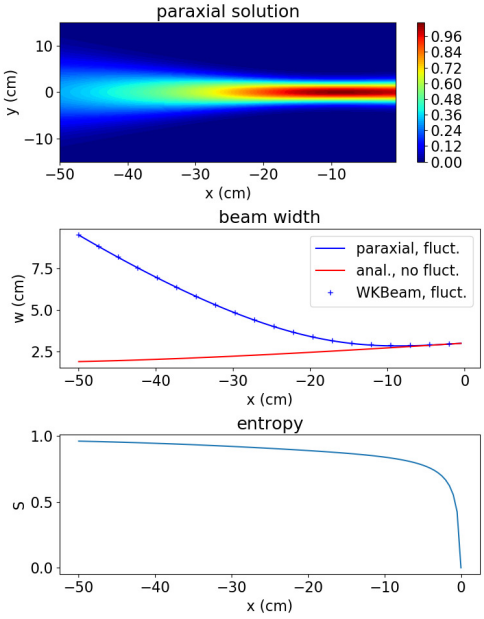

Figure 5. Initial beam width $w(0) = 3\,\mathrm{cm}$, initial beam curvature $R(0) = -100\,\mathrm{cm}$, beam frequency $f = 140\,\mathrm{GHz}$, fluctuation level $\delta = 0.05$, $L_F = 3\,\mathrm{cm}$. Top: Energy density of the paraxial solution, middle: comparison of the beam width of an analytical reference solution without fluctuation, WKBeam and the paraxial ansatz, bottom: entropy of the paraxial solution resolved in x.

References

[1] Bornatici M Cano R de Barbieri O Engelmann F 1983 Electron cyclotron emission and absorption in fusion plasmas *Nucl. Fusion* **23** 1153

[2] Tsironis C Peeters A G Isliker H Strintzi D Chatziantonaki I Vlahos L 2009 Electron-cyclotron wave scattering by edge density fluctuations in ITER *Phys. Plasmas* **16** 112510

[3] Snicker A Poli E Maj O Guidi L Köhn A Weber H Conway G Henderson M Saibene G2018 The effect of density fluctuations on electron cyclotron beam broadening and implications for ITER *Nucl. Fusion* **58** 016002

[4] Karal F Keller J 1964 Elastic, Electromagnetic, and Other Waves in a Random Medium *J. Math. Phys.* **5** 537

[5] Weber H Maj O Poli E 2015 Scattering of diffracting beams of electron cyclotron waves by random density fluctuations in inhomogeneous plasmas *EPJ Web Conf.* **87** 01002

[6] Graefe E-M Schubert R 2011 Wave-packet evolution in non-Hermitian quantum systems *Phys. Rev. A* **83** 060101

[7] Weber H 2013 Master thesis. *IPP report* 5/134, Max-Planck Institute for Plasma Physics, http://edoc.mpg.de

[8] Pereverzev G V 1998 Beam tracing in inhomogeneous anisotropic plasmas *Phys. Plasmas* **5** 3529

[9] Poli E Peeters A G Pereverzev G V 2001 TORBEAM, a beam tracing code for electron-cyclotron waves in tokamak plasmas *Comput. Phys. Commun.* **136** 90

[10] Poli E et al. 2018 TORBEAM 2.0, a paraxial beam tracing code for electron-cyclotron beams in fusion plasmas for extended physics applications *Comput. Phys. Commun.* **225** 36

[11] Ballentine L E 1970 The statistical interpretation of quantum mechanics. *Rev. Mod. Phys.* **42** 358

[12] Manfredi G Feix M R 2000 Entropy and Wigner functions *Phys. Rev. E*, **62** 4665